The Mechanics of
Earthquakes and Faulting

2nd edition

Christopher H. Scholz
Lamont–Doherty Geological Observatory and
Department of Earth and Environmental Sciences,
Columbia University

CAMBRIDGE
UNIVERSITY PRESS

PUBLISHED BY THE PRESS SYNDICATE OF THE UNIVERSITY OF CAMBRIDGE
The Pitt Building, Trumpington Street, Cambridge, United Kingdom

CAMBRIDGE UNIVERSITY PRESS
The Edinburgh Building, Cambridge CB2 2RU, UK
40 West 20th Street, New York, NY 10011–4211, USA
477 Williamstown Road, Port Melbourne, VIC 3207, Australia
Ruiz de Alarcón 13, 28014 Madrid, Spain
Dock House, The Waterfront, Cape Town 8001, South Africa

http://www.cambridge.org

First published 1990
First paperback edition 1990
Reprinted 1992, 1994, 1997, 2000
Second edition 2002

Printed in the United Kingdom at the University Press, Cambridge

Typeface Swift Regular 11/15 pt *System* QuarkXPress™ [SE]

A catalogue record for this book is available from the British Library

Library of Congress Cataloguing in Publication data

Scholz, C. H. (Christopher H.)
The mechanics of earthquakes and faulting / Christopher H. Scholz. – 2nd ed.
p. cm.
Includes bibliographical references and index.
ISBN 0-521-65223-5 (hardback) – ISBN 0-521-65540-4 (paperback)
1. Seismology. 2. Faults (Geology) I. Title.

QE534.2 .S37 2002
551.22–dc21 2001043297

ISBN 0 521 65223 5 hardback
ISBN 0 521 65540 4 paperback

Contents

1

Brittle fracture of rock

Under the low temperature and pressure conditions of Earth's upper lithosphere, silicate rock responds to large strains by brittle fracture. The mechanism of brittle behavior is by the propagation of cracks, which may occur on all scales. We begin by studying this form of deformation, which is fundamental to the topics that follow.

1.1 Theoretical concepts

1.1.1 *Historical*

Understanding the basic strength properties of rock has been a practical pursuit since ancient times, both because of the importance of mining and because rock was the principal building material. The crafting of stone tools required an intuitive grasp of crack propagation, and mining, quarrying, and sculpture are trades that require an intimate knowledge of the mechanical properties of rock. The layout and excavation of quarries, for example, is a centuries-old art that relies on the recognition and exploitation of preferred splitting directions in order to maximize efficiency and yield. One of the principal properties of brittle solids is that their strength in tension is much less than their strength in compression. This led, in architecture, to the development of fully compressional structures through the use of arches, domes, and flying buttresses.

Rock was one of the first materials for which strength was studied with scientific scrutiny because of its early importance as an engineering material. By the end of the nineteenth century the macroscopic phenomenology of rock fracture had been put on a scientific basis. Experimentation had been conducted over a variety of conditions up to moderate confining pressures. The Coulomb criterion and the Mohr circle analysis had been developed and applied to rock fracture with sufficient success that they

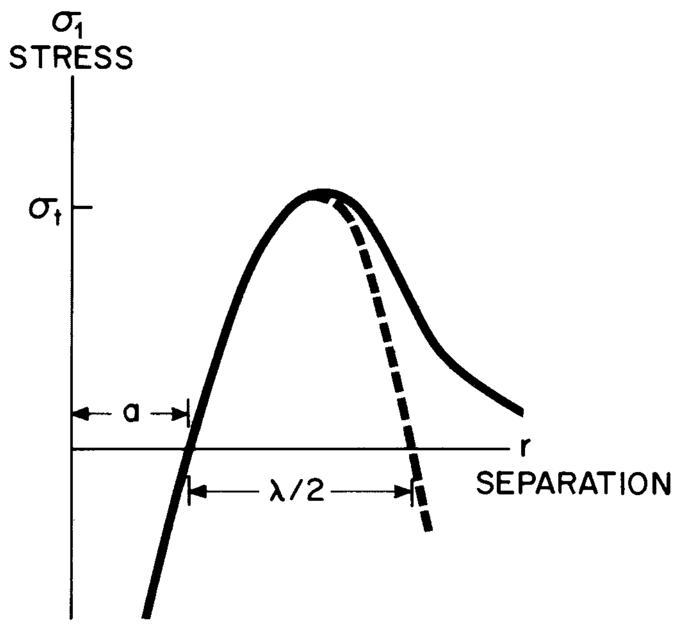

Fig. 1.1. Sketch of an anharmonic model of interatomic forces, showing the relationship between stress and atomic separation (solid curve) and a sinusoidal approximation (dashed curve).

remain the principal tools used to describe this process for many engineering and geological applications.

The modern theory of brittle fracture arose as a solution to a crisis in understanding the strength of materials, brought about by the atomic theory of matter. In simplest terms, strength can be viewed as the maximum stress that a material can support under given conditions. Fracture (or flow) must involve the breaking of atomic bonds. An estimate of the *theoretical strength* of a solid is therefore the stress required to break the bonds across a lattice plane.

Consider a simple anharmonic model for the forces between atoms in a solid, as in Figure 1.1, in which an applied tension σ produces an increase in atomic separation r from an equilibrium spacing a (Orowan, 1949). Because we need only consider the prepeak region, we can approximate the stress–displacement relationship with a sinusoid,

$$\sigma = \sigma_t \sin\left[\frac{2\pi(r-a)}{\lambda}\right] \tag{1.1}$$

For small displacements, when $r \approx a$, then

$$\frac{d\sigma}{d(r-a)} = \frac{E}{a} = \frac{2\pi}{\lambda}\sigma_t \cos\left[\frac{2\pi(r-a)}{\lambda}\right] \tag{1.2}$$

but because $(r-a)/\lambda \ll 1$, the cosine is equal to 1, and

$$\sigma_{\mathrm{t}} = \frac{E\lambda}{2\pi a} \tag{1.3}$$

where E is Young's modulus. When $r=3a/2$, the atoms are midway between two equilibrium positions, so by symmetry, $\sigma=0$ there and $a \approx \lambda$. The theoretical strength is thus about $E/2\pi$. The work done in separating the planes by $\lambda/2$ is the specific surface energy γ, the energy per unit area required to break the bonds, so

$$2\gamma = \int_0^{\lambda/2} \sigma_{\mathrm{t}} \sin\left[\frac{2\pi(r-a)}{\lambda}\right] d(r-a) = \frac{\lambda\sigma_{\mathrm{t}}}{\pi} \tag{1.4}$$

which, with $\sigma_{\mathrm{t}} \approx E/2\pi$, yields the estimate $\gamma \approx Ea/4\pi^2$.

The value of the theoretical strength from this estimate is 5–10 GPa, several orders of magnitude greater than the strength of real materials. This discrepancy was explained by the postulation and later recognition that all real materials contain defects. Two types of defects are important: cracks, which are surface defects; and dislocations, which are line defects. Both types of defects may propagate in response to an applied stress and produce yielding in the material. This will occur at applied stresses much lower than the theoretical strength, because both mechanisms require that the theoretical strength be achieved only locally within a *stress concentration* deriving from the defect. The two mechanisms result in grossly different macroscopic behavior. When cracks are the active defect, material failure occurs by its separation into parts, often catastrophically: this is brittle behavior. Plastic flow results from dislocation propagation, which produces permanent deformation without destruction of the lattice integrity.

These two processes tend to be mutually inhibiting, but not exclusive, so that the behavior of crystalline solids usually can be classed as brittle or ductile, although mixed behavior, known as semibrittle, may be more prevalent than commonly supposed. Because the lithosphere consists of two parts with markedly different rheological properties, one brittle and the other ductile, it is convenient to introduce two new terms to describe them. These are *schizosphere* (literally, the broken part) for the brittle region, and *plastosphere* (literally, the moldable part) for the ductile region. In this book we will assume, for the most part, that we are dealing with purely brittle processes, so that we will be concerned principally with the behavior of the schizosphere.

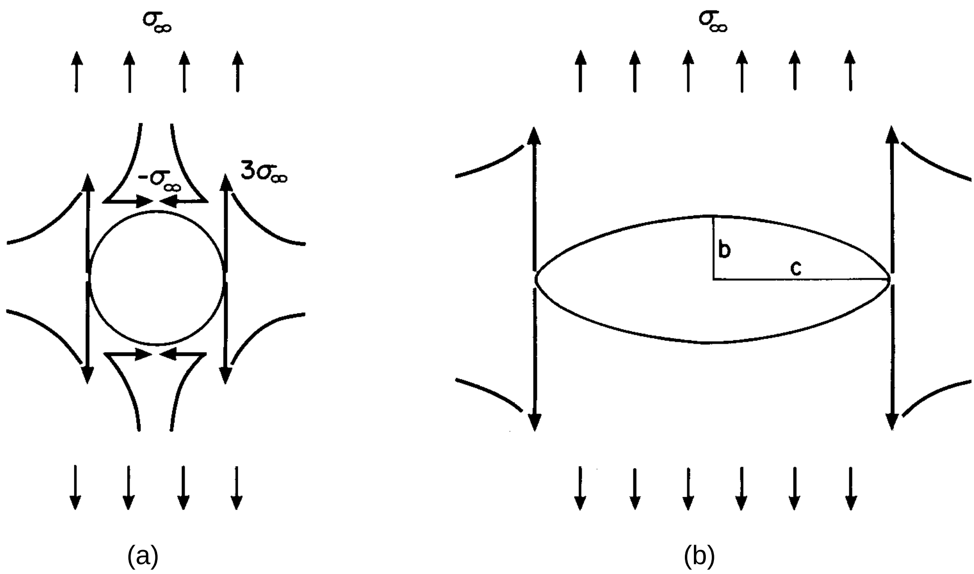

Fig. 1.2. Stress concentration around (a) a circular hole, and (b) an elliptical hole in a plate subjected to a uniform tension σ_∞.

1.1.2 *Griffith theory*

All modern theories of strength recognize, either implicitly or explicitly, that real materials contain imperfections that, because of the stress concentrations they produce within the body, result in failure at much lower stresses than the theoretical strength. A simple example, Figure 1.2(a), is a hole within a plate loaded with a uniform tensile stress σ_∞. It can be shown from elasticity theory that at the top and bottom of the hole a compressive stress of magnitude $-\sigma_\infty$ exists and that at its left and right edges there will be tensile stresses of magnitude $3\sigma_\infty$. These stress concentrations arise from the lack of load-bearing capacity of the hole and their magnitudes are determined solely by the geometry of the hole and not by its size. If the hole is elliptical, as in Figure 1.2(b), with semiaxes b and c, with $c>b$, the stress concentration at the ends of the ellipse increases proportionally to c/b, according to the approximate formula

$$\sigma \approx \sigma_\infty (1 + 2c/b)$$

or

$$\sigma \approx \sigma_\infty [1 + 2(c/\rho)^{1/2}] \approx \sigma_\infty (c/\rho)^{1/2} \tag{1.5}$$

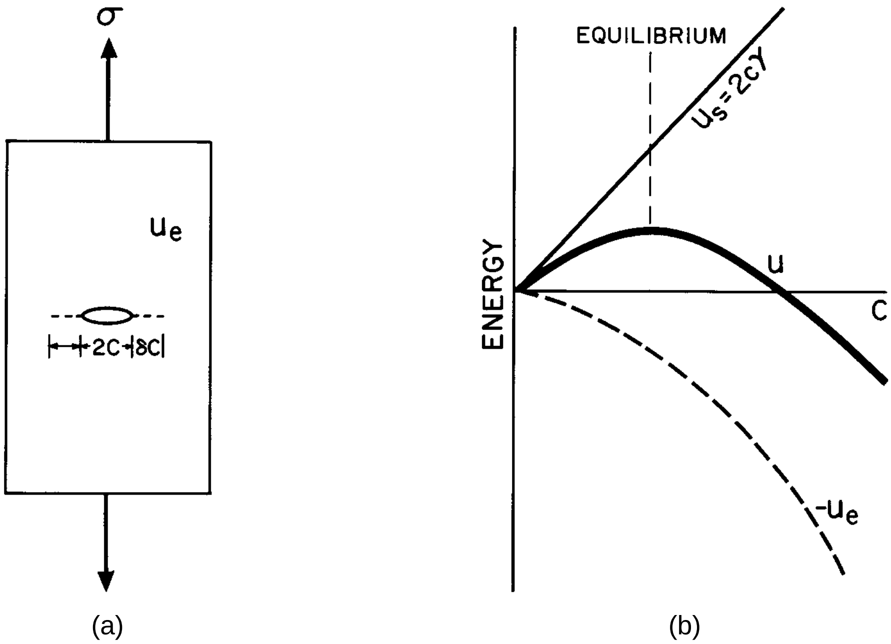

Fig. 1.3. Griffith's model for a crack propagating in a rod (a), and the energy partition for the process (b).

for $c \gg b$, where ρ is the radius of curvature at that point. It is clear that for a long narrow crack the theoretical strength can be attained at the crack tip when $\sigma_\infty \ll \sigma_t$. Because Equation (1.5) indicates that the stress concentration will increase as the crack lengthens, crack growth can lead to a dynamic instability.

Griffith (1920, 1924) posed this problem at a more fundamental level, in the form of an energy balance for crack propagation. The system he considered is shown in Figure 1.3(a) and consists of an elastic body that contains a crack of length $2c$, which is loaded by forces on its external boundary. If the crack extends an increment δc, work W will be done by the external forces and there will be a change in the internal strain energy U_e. There will also be an expenditure of energy in creating the new surfaces U_s. Thus the total energy of the system, U, for a static crack, will be

$$U = (-W + U_e) + U_s \tag{1.6}$$

The combined term in parentheses is referred to as the mechanical energy. It is clear that, if the cohesion between the incremental extension surfaces

δc were removed, the crack would accelerate outward to a new lower energy configuration: Thus, mechanical energy must decrease with crack extension. The surface energy, however, will increase with crack extension, because work must be done against the cohesion forces in creating the new surface area. There are two competing influences; for the crack to extend there must be reduction of the total energy of the system, and hence at equilibrium there is a balance between them. The condition for equilibrium is

$$dU/dc = 0 \tag{1.7}$$

Griffith analyzed the case of a rod under uniform tension. A rod of length y, modulus E, and unit cross section loaded under a uniform tension will have strain energy $U_e = y\sigma^2/2E$. If a crack of length $2c$ is introduced into the rod, it can be shown that the strain energy will increase an amount $\pi c^2\sigma^2/E$, so that U_e becomes

$$U_e = \sigma^2 (y + 2\pi c^2)/2E \tag{1.8}$$

The rod becomes more compliant with the crack, with an effective modulus $\underline{E} = yE/(y + 2\pi c^2)$. The work done in introducing the crack is

$$W = \sigma y(\sigma/\underline{E} - \sigma/E) = 2\pi\sigma^2 c^2/E \tag{1.9}$$

and the surface energy change is

$$U_s = 4c\gamma \tag{1.10}$$

Substituting Equations (1.8)–(1.10) into Equation (1.6) gives

$$U = -\pi c^2\sigma^2/E + 4c\gamma \tag{1.11}$$

and applying the condition for equilibrium (Equation (1.7)), we obtain an expression for the critical stress at which a suitably oriented crack will be at equilibrium,

$$\sigma_f = (2E\gamma/\pi c)^{1/2} \tag{1.12}$$

The energies of the system are shown in Figure 1.3(b), from which it can be seen that Equation (1.12) defines a position of unstable equilibrium: when this condition is met the crack will propagate without limit, causing macroscopic failure of the body.

Griffith experimentally tested his theory by measuring the breaking strength of glass rods that had been notched to various depths. He obtained an experimental result with the form of Equation (1.12) from which he was able to extract an estimate of γ. He obtained an independent estimate of γ by measuring the work necessary to pull the rods apart by necking at elevated temperatures. By extrapolating this result to room temperature, he obtained a value that was within reasonable agreement with that derived from the strength tests.

Griffith's result stems strictly from a consideration of thermodynamic equilibrium. Returning to our original argument, we may ask if the theoretical strength is reached at the crack tip when the Griffith condition is met: that is, is the stress actually high enough to break the bonds? This question was posed by Orowan (1949), who considered the stress at the tip of an atomically narrow crack, as described before. Combining Equations (1.3) and (1.4), we obtain

$$\sigma_{\mathrm{t}} = (E\gamma/a)^{1/2} \tag{1.13}$$

This stress will exist at the ends of a crack of length $2c$ when the macroscopic applied stress σ_{f} is (Equation (1.5))

$$\sigma_{\mathrm{t}} = 2\sigma_{\mathrm{f}}(c/a)^{1/2} \tag{1.14}$$

so that

$$\sigma_{\mathrm{f}} = (E\gamma/4c)^{1/2} \tag{1.15}$$

which is very close to Equation (1.12). The close correspondence of these two results demonstrates both necessary and sufficient conditions for crack propagation. Griffith's thermodynamic treatment shows the condition for which the crack is energetically favored to propagate, while Orowan's calculation shows the condition in which the crack-tip stresses are sufficient to break atomic bonds. For a typical value of $\gamma \approx Ea/30$ (Equation (1.4)), commonly observed values of strength of $E/500$ can be explained by the presence of cracks of length $c \approx 1$ μm. Prior to the advent of the electron microscope, the ubiquitous presence of such microscopic cracks was hypothetical, and this status was conferred upon them with the use of the term *Griffith crack.*

Griffith's formulation has an implicit instability as a consequence of the constant stress boundary condition. In contrast, the experiment of Obriemoff (1930) leads to a stable crack configuration. Obriemoff measured

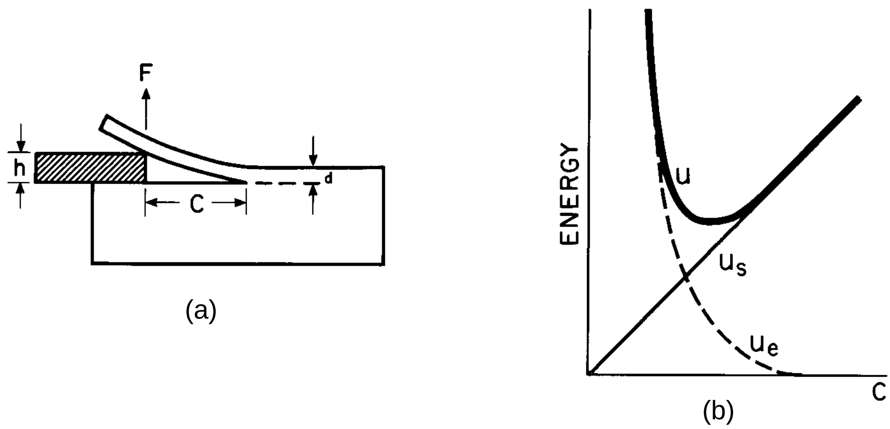

Fig. 1.4. The configuration of Obriemoff's mica cleaving experiment (a), and the energy partition for this process (b).

the cleavage strength of mica by driving a wedge into a mica book using the configuration shown in Figure 1.4(a). In this experiment the boundary condition is one of constant displacement. Because the wedge can be considered to be rigid, the bending force F undergoes no displacement and the external work done on the system is simply

$$W = 0 \tag{1.16}$$

From elementary beam theory, the strain energy in the bent flake is

$$U_e = Ed^3h^2/8c^3 \tag{1.17}$$

and, using $U_s = 2c\gamma$ and the condition $dU/dc = 0$, we obtain the equilibrium crack length

$$c = (3Ed^3h^2/16\gamma)^{1/4} \tag{1.18}$$

The energies involved in this system are shown in Figure 1.4(b). It is clear that in this case the crack is in a state of stable equilibrium; it advances the same distance that the wedge is advanced. This example shows that the stability is controlled by the system response, rather than being a material property, a point that will be taken up in greater detail in the discussion of frictional instabilities in Section 2.3. In this case the loading system may be said to be infinitely stiff, and crack growth is controlled and stable. Griffith's experiment, on the other hand, had a system of zero stiffness and the crack was unstable. Most real systems, however, involve loading systems with finite stiffness so that the stability has to be evaluated by balancing the rate at which work is done by the loading system against the energy absorbed by crack propagation.

Obriemoff noticed that the cracks in his experiment did not achieve their equilibrium length instantly, but that on insertion of the wedge they jumped forward and then gradually crept to their final length. When he conducted the experiment in vacuum, however, he did not observe this transient effect. Furthermore, the surface energy that he measured in vacuum was about 10 times the surface energy measured in ambient atmosphere. He was thus the first to observe the important effect of the chemical environment on the weakening of brittle solids and the *subcritical crack growth* that results from this effect. This effect is very important in brittle processes in rock and will be discussed in more detail in Section 1.3.2.

1.1.3 *Fracture mechanics*

Linear elastic fracture mechanics is an approach that has its roots in the Griffith energy balance, but that lends itself more readily to the solution of general crack problems. It is a continuum mechanics approach in which the crack is idealized as a mathematically flat and narrow slit in a linear elastic medium. It consists of analyzing the stress field around the crack and then formulating a fracture criterion based on certain critical parameters of the stress field. The macroscopic strength is thus related to the intrinsic strength of the material through the relationship between the applied stresses and the crack-tip stresses. Because the crack is treated as residing in a continuum, the details of the deformation and fracturing processes at the crack tip are ignored.

The displacement field of cracks can be categorized into three modes (Figure 1.5). Mode I is the tensile, or opening, mode in which the crack wall displacements are normal to the crack. There are two shear modes: in-plane shear, Mode II, in which the displacements are in the plane of the crack and normal to the crack edge; and antiplane shear, Mode III, in which the displacements are in the plane of the crack and parallel to the edge. The latter are analogous to edge and screw dislocations, respectively.

If the crack is assumed to be planar and perfectly sharp, with no cohesion between the crack walls, then the near-field approximations to the crack-tip stress and displacement fields may be reduced to the simple analytic expressions:

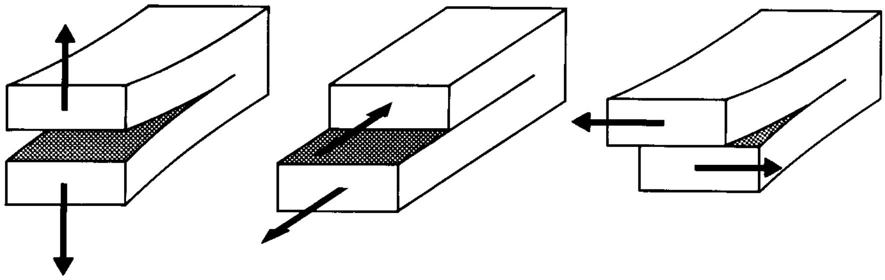

Fig. 1.5. The three crack propagation modes.

$$\sigma_{ij} = K_n(2\pi r)^{-1/2} f_{ij}(\theta) \tag{1.19}$$

and

$$u_i = (K_n/2E)(r/2\pi)^{1/2} f_i(\theta) \tag{1.20}$$

where r is the distance from the crack tip and θ is the angle measured from the crack plane, as shown in Figure 1.6. K_n is called the *stress intensity factor* and depends on mode, that is, K_I, K_{II}, and K_{III}, refer to the three corresponding crack modes. The functions $f_{ij}(\theta)$ and $f_i(\theta)$ can be found in standard references (e.g., Lawn and Wilshaw, 1975), and are illustrated in Figure 1.6. The stress intensity factors depend on the geometry and magnitudes of the applied loads and determine the intensity of the crack-tip stress field. They also can be found tabulated, for common geometries, in standard references (e.g., Tada, Paris, and Irwin, 1973). The other terms describe only the distribution of the fields.

In order to relate this to the Griffith energy balance it is convenient to define an *energy release rate*, or *crack extension force*,

$$\mathcal{G} = -d(-W + U_e)/dc \tag{1.21}$$

which can be related to K by (Lawn and Wilshaw, 1975, page 56)

$$\mathcal{G} = K^2/E \tag{1.22}$$

for plane stress or

$$\mathcal{G} = K^2(1-\nu^2)/E \tag{1.23}$$

for plane strain (ν is Poisson's ratio). In Mode III, the right-hand sides of the corresponding expressions must be multiplied by $(1+\nu)$ for plane stress and

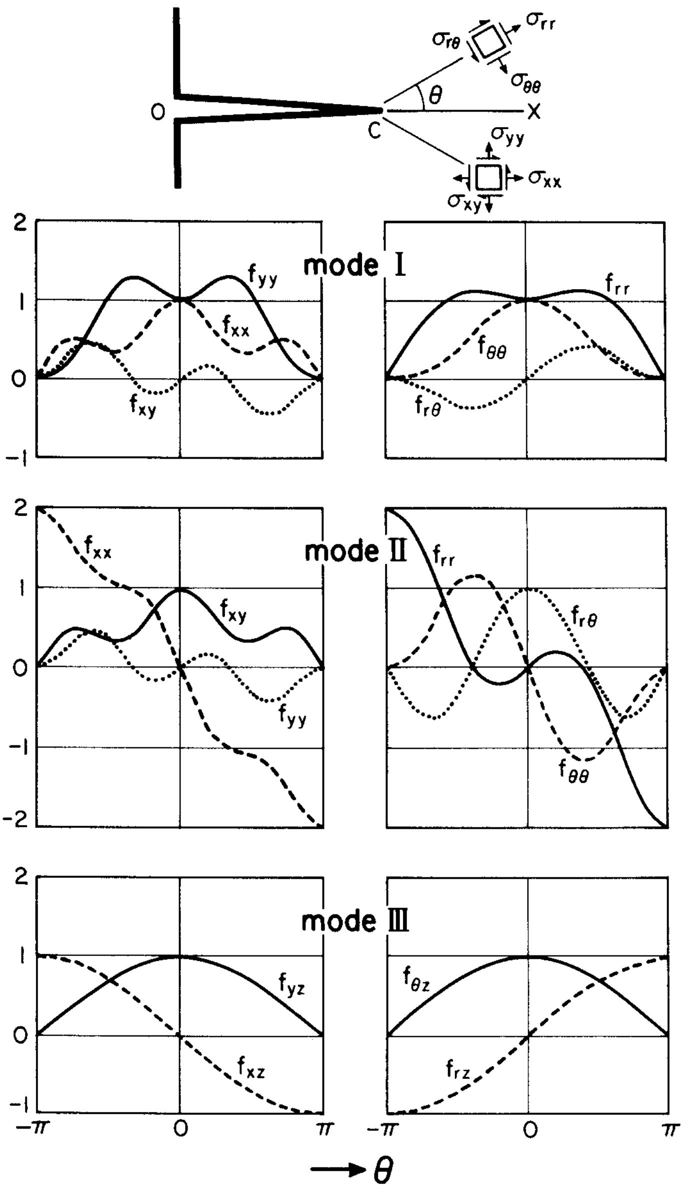

Fig. 1.6. The stress functions near the tips of the three modes of cracks, using both Cartesian and cylindrical coordinates, as shown in the geometrical key. (After Lawn and Wilshaw, 1975.)

divided by $(1-\nu)$ for plane strain, respectively. From Equations (1.6) and (1.7), it is clear that the condition for crack propagation will be met when

$$\mathcal{G}_c = \mathcal{K}_c^2/E = 2\gamma \tag{1.24}$$

for plane stress, with a corresponding expression for plane strain. Thus $\mathcal{K}_c$, the *critical stress intensity factor*, and $\mathcal{G}_c$ are material properties that, because

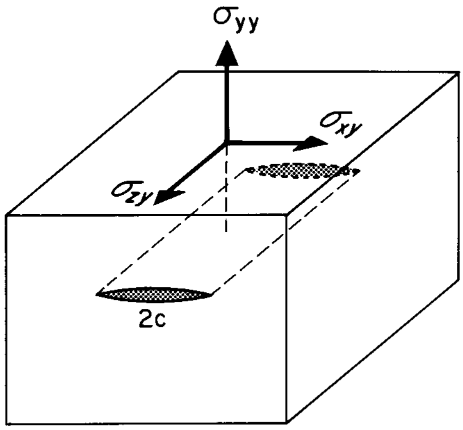

Fig. 1.7. Geometry of a crack in a uniform stress field.

they can be related to the applied stresses through a stress analysis, provide powerful and general failure criteria. $\mathcal{K}_c$ is also sometimes called the *fracture toughness*, and $\mathcal{G}_c$ the *fracture energy.*

A simple and useful case is when uniform stresses σ_{ij} are applied remote from the crack, as in Figure 1.7. In this case the stress intensity factors are given by

$$\left.\begin{aligned} K_{\mathrm{I}} &= \sigma_{yy}(\pi c)^{1/2} \\ K_{\mathrm{II}} &= \sigma_{xy}(\pi c)^{1/2} \\ K_{\mathrm{III}} &= \sigma_{zy}(\pi c)^{1/2} \end{aligned}\right\} \tag{1.25}$$

and, using Equation (1.22), the corresponding crack extension forces, for plane stress, are

$$\left.\begin{aligned} \mathcal{G}_{\mathrm{I}} &= (\sigma_{yy})^2 \pi c/E \\ \mathcal{G}_{\mathrm{II}} &= (\sigma_{xy})^2 \pi c/E \\ \mathcal{G}_{\mathrm{III}} &= (\sigma_{zy})^2 \pi c(1+\nu)/E \end{aligned}\right\} \tag{1.26}$$

In plane strain, E is relaced by $E/(1-\nu^2)$ for Modes I and II.

Equation (1.25) may be compared with the approximate expression for the stress concentration at the tip of an elliptical crack, Equation (1.5). However, inspection of Equation (1.19) indicates that there is a stress singularity at the crack tip. This results from the assumptions of perfect sharpness of the slit. This is nonphysical, both because it internally violates the assumption of linear elasticity, which implies small strains, and because no real material can support an infinite stress. There must be a region of nonlinear deformation near the crack tip that relaxes this singularity. This can be ignored in the fracture mechanics approach, because it can be shown that the strain energy in the nonlinear zone is bounded, and because the small nonlinear zone does not significantly distort the stress field at greater distances from the crack. It is, of course, of paramount importance for studies concerned with the detailed mechanics of crack advancement, but it suffices here to state that linear elastic fracture mechanics is not applicable at that scale or if there is large-scale yielding.

Within the nonlinear zone distributed cracking, plastic flow, and other dissipative processes may occur that contribute to the crack extension force. To account for these additional contributions we can rewrite Equation (1.24) as

$$\mathscr{G}_c = 2\Gamma \tag{1.27}$$

where Γ is a lumped parameter that includes all dissipation within the crack-tip region. This failure criterion is associated with the work of Irwin (1958). The fact that we do not usually know the specific processes that contribute to G is not normally of practical significance because $\mathscr{G}$ still can be evaluated if mechanical measurements can be made suitably outside the nonlinear zone (because integration around the crack tip is path-independent (Rice, 1968)).

A more serious problem, for geological applications, lies in the fracture mechanics assumption that the crack is cohesionless behind the crack tip. In shear motion on a fault, friction will exist over all the fault, and work done against this friction will become a significant term in an energy balance describing this process. As will be discussed in more detail in Section 4.2.1, it is not possible to evaluate this frictional work term and so solve for the energy partition in earthquakes. In terms of the present context, this means that, for the shear modes, Equations (1.24) and (1.27) are reduced to the status of local stress fracture criteria as opposed to global criteria tied to an energy balance.

1.1.4 *Crack models*

Faults and joints are naturally occurring shear and opening mode cracks, and earthquakes, which produce increments of slip within a limited area of a fault surface, may also be represented as shear cracks. Because we often have data on the relative displacements across such features, we wish to know the slip distributions expected from crack models and the relationship of those to the driving stresses. A crack model is one in which a stress drop is specified on a discontinuity within a stressed solid and the resulting displacements of the crack wall calculated. In fracture mechanics the cracks are assumed to be cohesionless and so the stress drop is equal to the applied stress. When applying such models to faults, we instead assume that the stress drop $\Delta\sigma$ is the applied stress less the residual friction stress on the fault. Notice the difference between a crack model and a dislocation model. In the latter the displacements on the discontinuity are specified, and the resulting deformations of the solid are calculated.

There are three types of crack models which we will consider in later chapters and which will therefore be introduced here.

Elastic crack model The theory of elastic cracks is treated in most standard textbooks in the theory of elasticity. A useful review with applications to geological problems is given by Pollard and Segall (1987). Consider a crack in an elastic body subjected to uniform stresses with the geometry shown in Figure 1.7. Relative displacements across the crack walls for the three crack modes are:

$$\begin{array}{l} \text{Mode I} \\ \text{Mode II} \\ \text{Mode III} \end{array} \quad \begin{Bmatrix} \Delta u_y \\ \Delta u_x \\ \Delta u_z \end{Bmatrix} = \begin{Bmatrix} \Delta\sigma_{yy} \\ \Delta\sigma_{xy} \\ \Delta\sigma_{zy} \end{Bmatrix} \frac{2(1-\nu)}{\mu}(c^2 - x^2)^{1/2} \tag{1.28}$$

Notice that the displacement distributions (Figure 1.8(a)) are elliptical for all modes, and their magnitudes increase linearly with the driving stresses and with the crack half-width c. The driving stress for the Mode I crack is the applied normal stress less the pore pressure in the crack, p. The driving stresses for the shear modes are the applied shear stresses less the residual friction stress σ_f. The displacement distribution for a circular crack of radius c is (Eshelby, 1957),

$$\Delta u(x, y) = \frac{24}{7\pi}\frac{\Delta\sigma}{\mu}[c^2 - (x^2 + y^2)]^{1/2} \tag{1.29}$$

Stress and displacement fields for elastic cracks are useful for analyzing crack interactions and are given, for selected cases, by Pollard and Segall (1987).

As noted in the previous section, these models have a stress singularity at

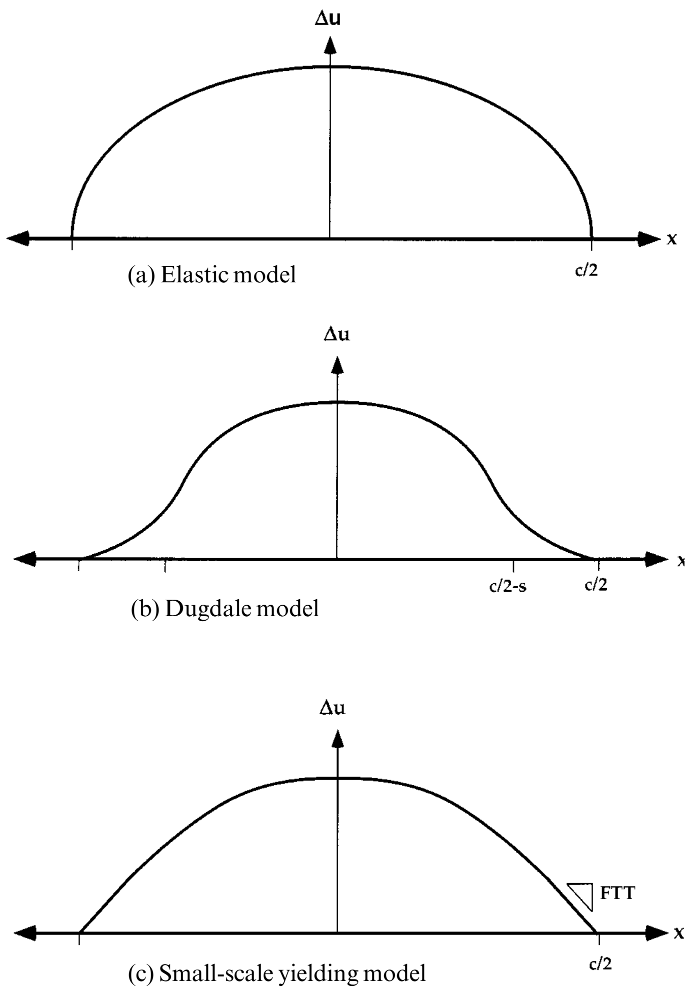

Fig. 1.8. The slip distributions for three types of crack models.

the crack tip. Therefore, they are not applicable in the vicinity of the crack tip. As will be noted in Section 3.2, displacement profiles for faults show a finite taper in the vicinity of the tip. This implies that some inelastic deformation has occurred near the fault tip to relax the stress singularity. Therefore, to study fault growth we need to examine crack models which include some yielding in the tip region. The next two models discussed were originally developed for the Mode I case (which is the main topic of engineering fracture mechanics). But, noting the above observation that the form of the displacement distribution does not depend on mode, here we discuss them in reference to the shear case.

Dugdale–Barenblatt model This model (Dugdale, 1960; Barenblatt, 1962) attempts to overcome the stress singularity problem of elastic crack models by assuming that there is a yielding, or breakdown region s on the plane of the crack in the vicinity of the tip. It does so by assuming that there is a cohesive stress, σ_y, equal to the yield strength of the material, which resists the crack driving stress in that region. For a shear crack with a residual friction stress σ_f, we substitute $(\sigma_0 - \sigma_f)$ for σ_y (Cowie and Scholz, 1992a). The displacement distribution on the crack is (Goodier and Field, 1963)

$$\Delta u = \frac{(1-v)(\sigma_0 - \sigma_f)c}{2\pi\mu}\left| \cos\theta \ln \frac{\sin^2(\theta_2 - \theta)}{\sin^2(\theta_2 + \theta)} + \cos\theta_2 \ln \frac{(\sin\theta_2 + \sin\theta)^2}{(\sin\theta_2 - \sin\theta)^2} \right| \tag{1.30}$$

where

$$\cos\theta = 2x/c \text{ for } |x| < c/2 \text{ and } \cos\theta_2 = (c - 2s)/c$$

This displacement distribution is shown in Figure 1.8(b). Displacements near the tip taper concavely towards the tip, maintaining the stresses in the breakdown region s at a constant finite value σ_0. Notice that, as in the elastic crack model, the displacement magnitudes scale linearly with stress drop $(\sigma_0 - \sigma_f)$ and with crack half-length. This model reduces to the elastic crack model in the limit that σ_0 tends to infinity.

The ogee form of this slip distribution is due to the contrived way in which the yielding is assumed to occur only on the plane of the crack. This form is seldom seen in real fault displacement profiles, which more often exhibit linear tapers in the tip region (Section 3.2). Furthermore, in Section 3.2 we also present evidence that inelastic deformation occurs within a volume surrounding fault tips. We need to consider, then, a model which contains those features.

CFTT model Numerical models have been investigated in which yielding is allowed to occur within a volume surrounding the crack tip. Such 'small-scale yielding' models (Kanninen and Popelar, 1985; Wang *et al.*, 1995) have displacement distributions as illustrated in Figure 1.8(c). The magnitude of the displacements scales in the same way as in the other crack models, but now the displacements taper linearly towards the tips. The slope of this taper is called the crack tip opening angle (CTOA) in the Mode I case, and here we will refer to it as the fault tip taper, FTT, for the shear case. It is found to be proportional to the yield strength of the material. A constant CTOA model most accurately duplicates experimental results of crack propagation in ductile materials such as stainless steel, where the CTOA is observed to be constant during crack growth and the J-resistance (a measure of $\mathcal{G}$) is observed to increase linearly with crack length. As we shall see in Section 3.2.2, both of these properties are observed for fault growth. Therefore, a constant FTT (or CFTT) model is the most realistic model for fault growth. Because these models cannot be expressed analytically, they have not found much use in the fault mechanics literature. Nevertheless, we will find it useful to use their properties in interpreting data regarding displacement gradients near fault tips.

1.1.5 *Macroscopic fracture criteria*

The theory of fracture discussed above specifies the conditions under which an individual crack will propagate in an elastic medium. We will show in Section 1.2, however, that only in one special case, that of tensile fracture of a homogeneous elastic material, do these theories also predict the macroscopic strength. In describing the strength of rock under general stress conditions, we are forced to use criteria which are empirical or semi-empirical. Such fracture criteria had been well established by the end of the nineteenth century and hence predate the theoretical framework that has been described so far.

In formulating a fracture criterion we seek a relationship between the principal stresses $\sigma_1 > \sigma_2 > \sigma_3$ (compression is positive) that defines a limiting failure envelope of the form

$$\sigma_1 = f(\sigma_2, \sigma_3) \tag{1.31}$$

with some parameters with which we can characterize the material.

One such criterion, which experiment shows is generally adequate, is that tensile failure will occur, with parting on a plane normal to the least principal stress, when that stress is tensile and exceeds some value T_0, the tensile strength. Thus,

$$\sigma_3 = -T_0 \tag{1.32}$$

Shear failure under compressive stress states is commonly described with the Coulomb criterion (often called the Navier–Coulomb, and sometimes the Coulomb–Mohr criterion). This evolved from the simple frictional criterion for the strength of cohesionless soils,

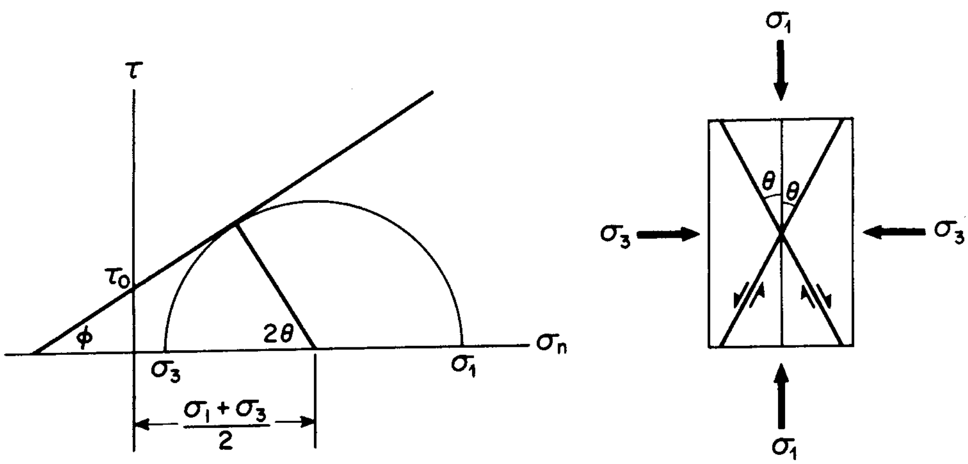

Fig. 1.9. Illustration of the Coulomb fracture criterion by means of a Mohr diagram. The relationships between the parameters at failure may be worked out from the geometry of the figure. On the right is shown the angular relationship between fracture planes and the principal stresses.

$$\tau = \mu\sigma_n \tag{1.33}$$

by the addition of a "cohesion" term τ_0. Thus

$$\tau = \tau_0 + \mu\sigma_n \tag{1.34}$$

where τ and σ_n are the shear and normal stresses resolved on any plane within the material. The parameter μ is called the *coefficient of internal friction* and is often written tan ϕ, ϕ being called the *angle of internal friction.* This criterion is shown in Figure 1.9, together with a Mohr circle from which the relationships between the failure planes and stresses can be deduced readily. From the Mohr circle it can be seen that failure will occur on two *conjugate* planes oriented at acute angles

$$\theta = \pi/4 - \phi/2 \tag{1.35}$$

on either side of the σ_1 direction and will have opposite senses of shear. From the geometry of Figure 1.9 one also can derive an expression of Equation (1.34) in principal axes, which, after some trigonometric manipulation, is found to be

$$\sigma_1[(\mu^2+1)^{1/2} - \mu] - \sigma_3[(\mu^2+1)^{1/2} + \mu] = 2\tau_0 \tag{1.36}$$

which is a straight line in the σ_1, σ_3 plane with intercept at the uniaxial compressive strength,

$$C_0 = 2\tau_0[(\mu^2 + 1)^{1/2} + \mu] \tag{1.37}$$

This criterion is defined only for compressive stresses. To form a complete criterion, we can specify this and combine Equation (1.36) with the tensile strength criterion, Equation (1.32) (Jaeger and Cook, 1976, pages 94–9):

$$\left.\begin{array}{l} \sigma_1[(\mu^2+1)^{1/2} - \mu] - \sigma_3[(\mu^2+1)^{1/2} + \mu] = 2\tau_0 \\ \text{when} \\ \sigma_1 > C_0[1 - C_0T_0/4\tau_0^2] \\ \text{and} \\ \sigma_3 = -T_0 \\ \text{when} \\ \sigma_1 < C_0[1 - C_0T_0/4\tau_0^2] \end{array}\right\} \tag{1.38}$$

This criterion is strictly two-dimensional: there is no predicted effect of the intermediate principal stress σ_2 on the strength.

The simple criterion for cohesionless soils, Equation (1.33), can be understood in terms of a microscopic failure process. The parameter μ is the friction coefficient between adjacent grains, which, in principle, can be determined independently of the criterion. Also, ϕ has a physical meaning: it is the steepest angle of repose that the material can support. In contrast, the coefficient of internal friction in the Coulomb criterion cannot be identified with any real friction coefficient, because the failure surface does not exist prior to failure. For the same reason, one cannot simply interpret the cohesion term as a pressure-independent strength that can be added simultaneously to this friction term. The Coulomb criterion thus may be viewed as strictly empirical.

Griffith (1924) developed a two-dimensional fracture criterion in terms of his theory of crack propagation. The underlying assumption of this criterion is that macroscopic failure can be identified with the initiation of cracking from the longest, most critically oriented Griffith crack. He analyzed the stresses around an elliptical crack in a biaxial stress field and found the most critical orientations that yielded the greatest tensile stress concentrations. He compared these results with that for a crack in uniaxial tension by normalizing them to the uniaxial tensile strength. The resulting criterion is

$$\left.\begin{array}{l} (\sigma_1 - \sigma_3)^2 - 8T_0(\sigma_1 + \sigma_3) = 0 \quad \text{if } \sigma_1 > -3\sigma_3 \\ \text{and} \\ \sigma_3 = -T_0 \text{ if } \sigma_1 < -3\sigma_3 \end{array}\right\} \tag{1.39}$$

The corresponding Mohr envelope is a parabola,

$$\tau^2 = 4T_0(\sigma_n + T_0) \tag{1.40}$$

(Jaeger and Cook, 1976, pages 94–9). For the tensile fracture portion of this failure envelope, the most critically oriented crack is normal to σ_3. For the shear portion, it is inclined at an angle θ from the σ_1 direction given by

$$\cos 2\theta = \tfrac{1}{2}(\sigma_1 - \sigma_3)/(\sigma_1 + \sigma_3)$$

This criterion is based on a microscopic failure mechanism. It has the attractive feature of combining tensile and shear failure in a single criterion. It predicts that $C_0 = 8T_0$, which, though smaller than generally observed, is of the correct order. Like the Coulomb criterion, it does not predict a σ_2 effect.

McClintock and Walsh (1962) pointed out that, under compressive stress states, cracks would be expected to close at some normal stress σ_c and thereafter crack sliding would be resisted by friction. They reformulated the Griffith criterion to admit this assumption and obtained the *modified Griffith criterion*

$$[(1 - \mu^2)^{1/2} - 1](\sigma_1 - \sigma_3) = 4T_0(1 + \sigma_c/T_0)^{1/2} + 2\mu(\sigma_3 - \sigma_c) \tag{1.41}$$

which has the corresponding Mohr envelope

$$\tau = 2T_0(1 + \sigma_c/T_0)^{1/2} + 2\mu(\sigma_n - \sigma_c) \tag{1.42}$$

This criterion, like the Coulomb criterion, predicts a linear relationship between the stresses. If we assume further that σ_c is negligibly small, we obtain the simplified forms

$$[(1 - \mu^2)^{1/2} - \mu](\sigma_1 - \sigma_3) = 4T_0 + 2\mu\sigma_3 \tag{1.43}$$

and

$$\tau = 2T_0 + \mu\sigma_n \tag{1.44}$$

which are identical with the Coulomb criterion, with $\tau_0 = 2T_0$, and μ now identified with the friction acting across the walls of preexisting cracks. This led Brace (1960) to suggest that this formed the physical basis for the Coulomb criterion.

These several criteria are compared in Figure 1.10 in (σ_1, σ_3) and (τ, σ_n) coordinates. They all, to an extent, account for the first-order strength prop-